22. *Space and Time Spectra of Stationary Stochastic Waves, with Special Reference to Microtremors.*

By Keiiti AKI,

Earthquake Research Institute.

(Read May 28, 1957.—Received June 30, 1957.)

Introduction

Since the days of Wiechert and Galitzin, seismograms have chiefly been investigated from the view point that they consist of successive distinguishable phases, and the travel time curves for various phases have been essential clues in revealing the structure and state of the matter within the earth. This idea of "phase" is indeed very natural and appropriate so far as the duration of shocks at their origin is negligibly short as compared with the characteristic time of the structure, such as a crustal layer, through which the seismic waves are propagated. Here the characteristic time of a layer may be represented by the ratio of its thickness to the velocity of seismic wave propagation in the layer.

There are, however, many cases in which the above assumption of short duration of shocks does not hold. An example of such cases is the propagation of seismic waves through a complicated crust. What can be clearly identified on the records of seismic waves due to near earthquakes such as those frequently observed in Japan is the initial motion of P waves and at best that of S waves. The main remaining part of such a seismogram has not been paid due attentions, if not neglected, any information from this source regarding the nature of the medium of propagation having been scarcely expected.

Other examples are the waves due to causes other than earthquakes, such as microseismic waves closely connected with meteorological disturbances, volcanic tremors, microtremors generated by traffic, and other tremors of artificial origin. It is hardly possible to deal with those waves from the standpoint of phases and to deduce from them any useful travel time curves.

The object of the present paper is to develop a method for dealing with those complicated waves in order that the nature of the waves as

well as the nature of the medium of propagation may be revealed. Since the method is based on a statistical investigation of waves in time and in space, we need to assume that our waves are stationary in both. This assumption represents quite an opposite extremity as compared with that underlying the phase method, and is certainly an appropriate one for studying those complicated waves mentioned above.

It is true that many studies on such waves have been made by various authors from the statistical point of view. But so far as the writer is aware, those studies have been made for rather limited purposes. For example, the study of spectral distribution of seismic waves has aimed at either getting useful information for earthquake damage prevention or investigating the dependence of the spectrum on the epicentral distance, the earthquake magnitude and the nature of wave paths and so on. Similar studies have also been made about volcanic tremors as well as microtremors due to traffic origin, and the spectrum of microseismic waves has been studied in reference to that of sea waves which are believed to cause them. Also the object of the use of filters in explosion seismology has been to secure a clearer identification of phases on a seismogram.

Those studies have been primarily concerned with the spectrum of waves in time, while the spectrum in space has not yet attracted due attentions. The recent study by K. Akamatsu[1] (1956) of the autocorrelation of microtremor waves in space is among the few made on the latter subject. She has made clear the spatial character of vibration of the ground. The process for obtaining the spatial autocorrelation coefficient, however, consists of troublesome steps such as simultanous recordings of vibrations at several points, readings of the recorded amplitudes, and computations of the autocorrelation coefficient among the waves to be studied. In order to secure rapidness and efficiency of measurments in the study of this kind, K. Aki[2] (1956) built a simple automatic computer by which the computation of spatial autocorrelation coefficients can be made without following individual steps stated above.

So far as the writer knows, the study to be reported here is the first, specifically designed to elucidate the relation between the spectrum of waves in space and that in time with reference to the nature of medium of propagation. By means of the method presented in this paper, the direction distribution of propagation as well as the mode of

1) K. AKAMATU, *Zisin*, [ii], **9** (1956), 22.
2) K. AKI, *ibid.* **9** (1956), 40.

polarization of complicated waves can be learned as will be seen in later chapters. Also we can obtain the dispersion curves for those waves which are useful for deducing the structure of the medium. In addition to this, if the waves observed consist of partial waves having different velocities, the power of each waves can be found.

In Chapter 1 will be given, some results of theoretical considerations of stochastic waves which are stationary both in time and space, and it will be shown what should be measured in order to find the dispersion curves, the mode of polarization, etc. of the waves. The instruments designed specifically for this purpose will be described in Chapter 2. They consists of filters of phase shift type and an automatic computer of the correlation coefficient.

Chapter 3 will be devoted to describing the results of application of the present method to the study of microtremors due to traffic observed at Hongo, Tokyo. The results obtained are as follows; 1) those waves are propagating in every direction with almost uniform power; 2) the horizontal component of vibration is strongly polarized in the direction prependicular to the direction of propagation showing that they are of Love type; 3) the dispersion curves have been deduced, and the velocities of S waves at various depths calculated.

Chapter 1. Theory of stationary stochastic waves

The most fundamental material in the study of wave from the standpoint of phases is certainly the travel time curve which indicates the relation between the treval time and epicentral distance. It may be expected that the corresponding fundamental material in the spectral studies of waves will be a certain relation between the spectrum of the waves in space and that in time. At first we shall look for this relation in the most simplified case of one dimensional waves, and at the same time shall attempt to show the characteristics of stochastic waves which are stationary in time and space.

1. One dimensional stationary waves having one single velocity

With the assumption that our waves travel with a single and definite velocity c independent of the frequency of vibration, our waves $u(x, t)$ can be expressed for the region $x=0 \sim X$ formally

$$u(x,\ t)=\sum A_n \exp(i\rho_n x)\cos c\rho_n t + \sum \frac{B_n}{c\rho_n}\exp(i\rho_n x)\sin c\rho_n t \qquad (1)$$

where

$$\rho_n = 2\pi\frac{n}{X} \quad (n=0,\ \pm 1,\ \pm 2,\ \cdots)$$

This is the solution of the one dimensional wave equation under the initial conditions that

$$\left.\begin{aligned} u(x,\ 0)&=\sum A_n \exp(i\rho_n x) \\ \dot{u}(x,\ 0)&=\sum B_n \exp(i\rho_n x)\,. \end{aligned}\right\} \qquad (2)$$

Since $u(x,\ 0)$ and $\dot{u}(x,\ 0)$ are both real, A_n and B_n must be the conjugate complex numbers of A_{-n} and B_{-n} respectively.

Now let us find the condition under which the waves formally given by Eq. (1) are stationary both in time and in space. At first, we notice the initial state of our waves as given by Eq. (2). Here $u(x,\ 0)$ and $\dot{u}(x,\ 0)$ should be treated as stochastic variables with a parameter x.

The Fourier coefficient A_n of a general stochastic process which is stationary with respect to a single parameter x for the region $x=0\sim X$ is known to be written in terms of the corresponding Fourier coefficient E_n of the so called "thermal or white noise" as follows;

$$A_n = E_n^{(A)}\cdot G^{(A)}(\rho_n)\,, \qquad (3)$$

where $G^{(A)}(\rho_n)$ is not a stochastic variable. From the purely random character of "white noise", it follows that

$$\left.\begin{aligned} \overline{E_n\cdot E_m}&=0\,, \quad n+m\neq 0\,, \\ \overline{E_n\cdot E_{-n}}&=\overline{|E_n|^2}=\frac{\Delta\rho_n}{2\pi}=\frac{1}{X}\,, \end{aligned}\right\} \qquad (4)$$

where the bars represent the operation of average.

Using these formulas, we have

$$\left.\begin{aligned} &\overline{A_nA_m}=0\,, \quad n+m\neq 0\,,\\ &\overline{|A_n|^2}=|G^{(A)}(\rho_n)|^2\frac{\Delta\rho_n}{2\pi}\,,\end{aligned}\right\} \tag{5}$$

and in a similar way,

$$\left.\begin{aligned} &\overline{B_nB_m}=0\,, \quad n+m\neq 0\\ &\overline{|B_n|^2}=|G^{(B)}(\rho_n)|^2\frac{\Delta\rho_n}{2\pi}\,.\end{aligned}\right\}$$

These are the statistical relations existing among the Fourier coefficients A_n's and B_n's. Moreover, if the initial distributions of displacement and that of velocity are independent of each other, we have

$$\overline{A_nB_m}=0\,, \tag{6}$$

for all n and m. From Eqs. (2) and (5), we see that $|G^{(A)}(\rho_n)|^2$ and $|G^B(\rho_n)|^2$ represent the spatial spectrum density of the initial displacement and that of the initial velocity respectively.

Defining the spatial autocorrelation function $\phi(\xi,\ t)$ of our waves for a given time t as

$$\phi(\xi,\ t)=\overline{u(x,\ t)u(x+\xi,\ t)} \tag{7}$$

and using Eqs. (5) and (6), we obtain

$$\begin{aligned}\phi(\xi,\ t)&=\sum\frac{\Delta\rho_n}{2\pi}\left\{|G^A(\rho_n)|^2\cos^2 c\rho_nt+\frac{|G^B(\rho_n)|^2}{c^2\rho_n^2}\sin^2 c\rho_nt\right\}\exp(i\rho_n\xi)\\ &=\frac{1}{2\pi}\int\{|G^A(\rho_n)|^2\cos^2 c\rho_nt+\frac{|G^B(\rho_n)|^2}{c^2\rho_n^2}\sin^2 c\rho_nt\}\exp(i\rho_n\xi)d\rho\end{aligned} \tag{8}$$

From Eq. (8), we see that if

$$\left.\begin{aligned} &|G^A(\rho_n)|^2=\frac{|G^B(\rho_n)|^2}{c^2\rho_n^2}\\ \text{or}\qquad &\\ &\omega_n^2|A_n|^2=|B_n|^2\,,\end{aligned}\right\} \tag{9}$$

where ω_n is the circular frequency and $\omega_n=c\rho_n$, $\phi(\xi,\ t)$ becomes independent of time. Thus we can reasonably take Eq. (9) as the condition for stationary stochastic waves. Eq. (9) can be considered as representing the law of equipartition of energy in the case of stochastic waves.

Introducing this condition into Eq. (8) and dropping the suffix A we get

$$\phi(\xi,\ t) \equiv \phi(\xi)=\frac{1}{2\pi}\int |G(\rho)|^2 \exp(i\rho\xi)d\rho \tag{10}$$

We shall now proceed to investigate the relation between the spectrum in space and that in time. For this we define the spectrum density in time as

$$\Phi(\omega_n)=\frac{1}{4}\cdot\frac{\overline{\{U_c(\omega_n)\}^2}+\overline{\{U_s(\omega_n)\}^2}}{\Delta\omega_n/2\pi} \tag{11}$$

where $U_c(\omega_n)$ is the Fourier cosine coefficient of $u(x,\ t)$ with respect to t and for a given x, while $U_s(\omega_n)$ is the corresponding sine coefficient. It can readily be seen from Eq. (1) that

$$\left.\begin{aligned} U_c(\omega_n)&=A_n\exp\left(i\frac{\omega_n}{c}x\right)+A_{-n}\exp\left(-i\frac{\omega_n}{c}x\right)\\ U_s(\omega_n)&=\frac{B_n}{\omega_n}\exp\left(i\frac{\omega_n}{c}x\right)+\frac{B_{-n}}{\omega_n}\exp\left(-i\frac{\omega_n}{c}x\right)\end{aligned}\right\} \tag{12}$$

and

$$\Delta\omega_n=c\Delta\rho_n=\frac{2\pi c}{X}$$

Inserting Eq. (12) into Eq. (11), we get

$$\Phi(\omega_n)=$$

$$\frac{\left[A_n\exp\left(i\frac{\omega_n}{c}x\right)+A_{-n}\exp\left(-i\frac{\omega_n}{c}x\right)\right]^2+\left[\frac{B_n}{\omega_n}\exp\left(i\frac{\omega_n}{c}x\right)+\frac{B_{-n}}{\omega_n}\exp\left(-i\frac{\omega_n}{c}x\right)\right]^2}{4\Delta\omega_n/2\pi}$$

By the use of Eq. (5) this may be written as

$$\Phi(\omega_n)=\frac{2\overline{A_nA_{-n}}+2\overline{B_nB_{-n}}/\omega_n^2}{4\Delta\omega_n/2\pi}$$

Finally, inserting Eq. (9) into this, we obtain the following equation,

$$\Phi(\omega)=\frac{|G(\rho)|^2\Delta\rho/2\pi}{\Delta\omega/2\pi}=\frac{|G(\omega/c)|^2}{c} \tag{14}$$

where the suffix n is dropped. This is the relation which connects the spectrum density in space and that in time in the case of one dimensional waves.

As will be shown later, as compared with Eq. (14), the following equation which relates the spatial autocorrelation function $\phi(\xi)$ with the spectrum density $\Phi(\omega)$ in time is more convenient for the purpose of the present study,

$$\phi(\xi)=\frac{1}{2\pi}\int_{-\infty}^{\infty}\Phi(\omega)\exp\left(i\frac{\omega}{c}\xi\right)d\omega$$

or (15)

$$\phi(\xi)=\frac{1}{\pi}\int_{0}^{\infty}\Phi(\omega)\cos\left(\frac{\omega}{c}\xi\right)d\omega$$

which can readily be obtained by Eqs. (10) and (14).

2. Dispersive waves

We shall now proceed to the case of dispersive waves, and show that Eq. (15) obtained above holds also in this case without any modification except the substitution of the function $c(\omega)$ of frequency ω for the constant velocity c. For this, we notice that if we take $\Delta\rho_n$ as constant for all n, the interval $\Delta\omega_n$ between consecutive ω_n is no longer constant in the dispersive case and varies with n. Then we may write

$$\Delta\omega_n=\left(\frac{d\omega}{d\rho}\right)_n\Delta\rho_n\,. \tag{16}$$

The equation corresponding to Eq. (14) is now written as

$$\Phi(\omega)=\frac{|G(\omega/c)|^2}{d\omega/d\rho}\,. \tag{17}$$

Introducing of this into Eq. (10) yields the final formula,

$$\phi(\xi)=\frac{1}{2\pi}\int_{-\infty}^{\infty}|G(\omega/c)|^2\exp\left(\frac{i\omega}{c(\omega)}\xi\right)\frac{d\rho}{d\omega}\,d\omega$$
$$=\frac{1}{\pi}\int_0^{\infty}\Phi(\omega)\cos\left(\frac{\omega}{c(\omega)}\xi\right)d\omega \qquad (18)$$

3. Spatial autocorrelations of filtered waves (1)

In this section the most essential part of our method will be illustrated in the case of one dimensional waves. Corresponding to the separation of a seismogram into successive particular phases in a study of "phases", the vibration of a seismograph is resolved into simple harmonic oscillations; in other words, a Fourier analysis is applied to the vibration in this method. For this purpose, we use electronic resonators to which we shall refer in Chapter 2. If the filtration by a resonator having frequency ω_0 is sufficiently sharp to allow us to assume the spectrum density of the filtered vibration to be

$$\Phi(\omega)=P(\omega_0)\delta(\omega-\omega_0)\,,\quad \omega>0 \qquad (19)$$

where $\delta(\omega)$ is the Dirac δ-function, then the corresponding spatial autocorrelation function (18) is written as

$$\phi(\xi,\,\omega_0)=P(\omega_0)\cos\left(\frac{\omega_0}{c(\omega_0)}\xi\right). \qquad (20)$$

Defining the autocorrelation coefficient as

$$\rho(\xi,\,\omega_0)\equiv\frac{\phi(\xi,\,\omega_0)}{\phi(0,\,\omega_0)}\,,$$

we may write it as

$$\rho(\xi,\,\omega_0)=\cos\left(\frac{\omega_0}{c(\omega_0)}\xi\right). \qquad (21)$$

The above formula shows that the dispersion curve i.e. the curve of velocity $c(\omega_0)$ as a function of frequency ω_0 can be obtained directly from the measurement of $\rho(\xi,\,\omega_0)$. The measurement of this quantity $\rho(\xi,\,\omega_0)$ for various frequencies ω_0 and for a fixed distance ξ is therefore the most fundamental in our method. But this is allowed only in the case in which the waves concerned have a single velocity corresponding

to a frequency ω.

Next, we shall consider the wave which is composed of partial waves having different velocities. In this case if we are allowed to assume that the component waves are statistically independent of one another, we can separate the composite waves into the components by measuring $\rho(\xi, \omega_0)$. Now we write the quantities related to the n'th component wave by attaching the suffix n: for instance, the displacement of the n'th component as $u_n(x, t)$ and the corresponding velocity as $c_n(\omega)$. Then from the assumption of independence among the components, it follows that

$$u(x, t)=\sum_n u_n(x, t)\,,$$

$$\phi(\xi)=\sum_n \phi_n(\xi)=\sum \frac{1}{2\pi}\int \Phi_n(\omega)\exp\left(i\frac{\omega}{c_n(\omega)}\xi\right)d\omega\,,$$

$$\phi(\xi, \omega_0)=\sum_n P_n(\omega_0)\cos\left(\frac{\omega_0}{c_n(\omega_0)}\xi\right)\,,$$

$$\rho(\xi, \omega_0)=\sum_n \frac{P_n(\omega_0)}{P(\omega_0)}\cos\left(\frac{\omega_0}{c_n(\omega_0)}\xi\right)\,. \tag{22}$$

The last equation shows that the number N of components is, finite, we can in principle obtain both the percentage of power of the n'th component and the corresponding velocity from the value of $\rho(\xi, \omega_0)$ for a given ω_0 and for $(2N-1)$ different ξ's.

Finally, there may be cases in which the wave can be assumed as composed of component waves having continuously distributed velocity. In this case, introducing the velocity distribution function defined as

$$p(\omega, c)=P_n(\omega)/\Delta c_n$$

and replacing the summation by the integration in Eq. (22), we have

$$\rho(\xi, \omega)=\frac{1}{P(\omega)}\int_0^\infty p(\omega, c)\cos\left(\frac{\omega}{c(\omega)}\xi\right)dc\,. \tag{23}$$

From this and using the Fourier transformation, we obtain

$$\frac{c^2 p(\omega, c)}{P(\omega)}=\frac{2}{\pi}\int_0^\infty \rho(\xi, \omega)\cos\left(\frac{\omega}{c(\omega)}\xi\right)d\xi\,. \tag{24}$$

Therefore, if we find the values of $\rho(\xi, \omega)$ for $\xi=0\sim\infty$, we can calculate the percentage of power of component wave having the assigned velocity and frequency contained in the wave in question.

4. Two dimensional waves of a single velocity

Now let us investigate the case of two dimensional waves, in which the reasonning is quite analogous to that given above for the case of one dimensional waves, though there appear additional terms such as the direction of propagation and polarization of vibrations. At first we shall deal with those waves which are neither dispersive nor polarized.

Assuming that our waves travel with a single velocity c, we write them in the form

$$u(x, y, t)=\sum\sum A_{nm}\exp(i\rho_n x\cos\theta_m+i\rho_n y\sin\theta_m)\cos(c\rho_n t)+\sum\sum\frac{B_{nm}}{c\rho_n}\exp(i\rho_n x\cos\theta_m+i\rho_n y\sin\theta_m)\sin(c\rho_n t)\,. \quad (25)$$

This is the solution of a two dimensional wave equation under the initial conditions that

$$\left.\begin{aligned} u(x, y, 0)&=\sum\sum A_{nm}\exp(i\rho_n x\cos\theta_m+i\rho_n y\sin\theta_m)\\ \dot{u}(x, y, 0)&=\sum\sum B_{nm}\exp(i\rho_n x\cos\theta_m+i\rho_n y\sin\theta_m)\end{aligned}\right\}\,. \quad (26)$$

Since $u(x, y, 0)$ and $\dot{u}(x, y, 0)$ are both real, $A_{n,m}$ and $B_{n,m}$ are the conjugate complex number of $A_{n,m+(\pi)}$ and $B_{n,m+(\pi)}$ respectively, in which (π) is a suffix defined by the relation, $\theta_{(\pi)}=\pi$.

Analogous to Eq. (5), the mean value of the absolute square of $A_{n,m}$ and that of $B_{n,m}$ are written as

$$\left.\begin{aligned}\overline{|A_{nm}|^2}&=|G^A(\rho_n, \theta_m)|^2\frac{\rho_n\Delta\theta_m\Delta\rho_n}{(2\pi)^2}\\ \overline{|B_{nm}|^2}&=|G^B(\rho_n, \theta_m)|^2\frac{\rho_n\Delta\theta_m\Delta\rho_n}{(2\pi)^2}\end{aligned}\right\}\,. \quad (27)$$

The spectrum density $|G(\rho, \theta)|^2$ in the above equation represents the amount of power carried in the waves at the initial state per unit area of the phase space which is formed by two dimensional wave numbers $\lambda=\rho\cos\theta$ and $\mu=\rho\sin\theta$.

Again corresponding to Eq. (5), we have

$$\left.\begin{aligned}&\overline{A_{nm}\cdot A_{n'm'}}=0\,,\quad n\neq n',\ m\neq m'\pm(\pi)\\&\overline{B_{nm}\cdot B_{n'm'}}=0\,,\quad n\neq n',\ m\neq m'\pm(\pi)\end{aligned}\right\}\tag{28}$$

and corresponding to Eq. (6),

$$\overline{A_{nm}B_{n'm'}}=0\tag{29}$$

for all n, m, n' and m'.

Using the above formulas we can write the spatial autocorrelation function $\phi(\xi, \eta, t)$ for the two dimensional waves in terms of their spectrum density in space as

$$\begin{aligned}\phi(\xi,\eta,t)&\equiv\overline{u(x,y,t)u(x+\xi,\ y+\eta,\ t)}\\&=\sum\sum\frac{\rho_n\Delta\rho_n\Delta\theta_m}{(2\pi)^2}\left\{|G^A(\rho_n,\ \theta_m)|^2\cos^2(c\rho_n t)\right.\\&\quad\left.+\frac{|G^B(\rho_n,\ \theta_m)|^2}{c^2\rho_n^2}\sin^2(c\rho_n t)\right\}\exp(i\rho_n\xi\cos\theta_m+i\rho_n\eta\sin\theta_m)\end{aligned}$$

From the above equation, it follows that the condition for a stationary stochastic wave of two dimensions is written as

$$\left.\begin{aligned}&|G^A(\rho,\ \theta)|^2=\frac{|G^B(\rho,\ \theta)|^2}{c^2\rho^2}\\\text{or}\qquad&\\&\omega_n^2\overline{|A_{nm}|^2}=\overline{|B_{nm}|^2}\end{aligned}\right\}.\tag{30}$$

Introducing this into $\phi(\xi, \eta, t)$, we obtain

$$\phi(\xi,\eta,t)\equiv\phi(\xi,\eta)=\sum\sum\frac{\rho_n\Delta\rho_n\Delta\theta_m}{(2\pi)^2}|G^A(\rho_n,\ \theta_m)|^2\exp(i\rho_n\xi\cos\theta_m+i\rho_n\eta\sin\theta_m)$$

Replacing the summation by the integration and dropping the suffix A we have

$$\phi(\xi,\eta)=\frac{1}{(2\pi)^2}\iint|G(\rho,\ \theta)|^2\exp(i\rho\xi\cos\theta+i\rho\eta\sin\theta)\rho d\rho d\theta\tag{31}$$

and accordingly we also have by the Fourier transformation

$$|G(\rho,\ \theta)|^2=\iint\phi(\xi,\eta)\exp(-i\rho\xi\cos\theta-i\rho\eta\sin\theta)d\xi d\eta\tag{32}$$

On the other hand, the spectrum density in time of the wave is written as

$$\Phi(\omega_n)=\frac{1}{4}\cdot\frac{\overline{(U_c(\omega_n))^2}+\overline{(U_s(\omega_n))^2}}{\Delta\omega_n/2\pi} \tag{33}$$

where $U_c(\omega_n)$ is the Fourier cosine coefficient of $u(x, y, t)$ with respect to t for given x and y, while $U_s(\omega_n)$ is the corresponding sine coefficient. We see in Eq. (25) that

$$\left.\begin{aligned} U_c(\omega_n)&=\sum_m A_{nm}\exp\left(i\frac{\omega_n}{c}x\cos\theta_m+i\frac{\omega_n}{c}y\sin\theta_m\right)\\ U_s(\omega_n)&=\sum_m \frac{B_{nm}}{\omega_n}\exp\left(i\frac{\omega_n}{c}x\cos\theta_m+i\frac{\omega_n}{c}y\sin\theta_m\right)\\ \omega_n&=c\rho_n\,. \end{aligned}\right\} \tag{34}$$

Using Eqs. (27), (28), (30), and (32), we can write the spectrum density $\Phi(\omega)$ in terms of the spatial autocorrelation function $\phi(\xi, \eta)$ as follows,

$$\begin{aligned}\Phi(\omega_n)&=\frac{\sum_m \overline{|A_{nm}|^2}+\overline{|B_{nm}|^2}/\omega_n^2}{4\Delta\omega_n/2\pi}\\ &=\frac{1}{4\pi c}\int_0^{2\pi}\left|G\left(\frac{\omega_n}{c},\ \theta\right)\right|^2\frac{\omega_n}{c}d\theta\\ &=\frac{1}{4\pi c}\int_0^{2\pi}\frac{\omega_n}{c}d\theta\iint\phi(\xi,\ \eta)\exp\left(-i\frac{\omega_n}{c}\xi\cos\theta-i\frac{\omega_n}{c}\eta\sin\theta\right)d\xi d\eta\,.\end{aligned} \tag{35}$$

Replacing (ξ, η) by a circular coordinate (r, ψ) defined as

$$\xi=r\cos\psi$$

$$\eta=r\sin\psi$$

and using the relation

$$\int_0^{2\pi}d\theta\exp\{-i\rho r\cos(\theta-\psi)\}=2\pi J_0(\rho r)$$

we have from Eq. (35)

$$\Phi(\omega)=\frac{1}{2c}\iint\phi(r,\ \psi)J_0(\rho r)\frac{\omega}{c}drd\psi\,. \tag{36}$$

If we introduce the azimuthal average of the spatial autocorrelation function, i.e.

$$\overline{\phi}(r)=\frac{1}{2\pi}\int\phi(r,\ \psi)d\psi \tag{37}$$

we see that a one to one correspondence exists between this function $\overline{\phi}(r)$ and the spectrum density $\Phi(\omega)$ as follows

$$\Phi(\omega)=\frac{\pi}{c^2}\omega\int_0^\infty\overline{\phi}(r)J_0\left(\frac{\omega}{c}r\right)rdr \tag{38}$$

$$\overline{\phi}(r)=\frac{1}{\pi}\int_0^\infty\Phi(\omega)J_0\left(\frac{\omega}{c}r\right)d\omega \tag{39}$$

This last equation (39) is derived by the use of the Hankel transformation. It is clear that Eq. (39) corresponds to Eq. (15) for one dimensional waves.

5. Dispersive waves of two dimensions

It will be shown in this section that Eq. (39) also holds in the case of dispersive waves without modifications except the substitution of the function $c(\omega)$ of frequency ω for the constant velocity c.

Taking the relation into account,

$$\Delta\omega_n=\left(\frac{d\omega}{d\rho}\right)_n\Delta\rho_n$$

we obtain

$$\Phi(\omega)=\frac{1}{4\pi}\frac{d\rho}{d\omega}\int_0^{2\pi}\left|G\left(\frac{\omega}{c},\theta\right)\right|^2\frac{\omega}{c}d\theta$$

corresponding to Eq. (35) of non-dispersive waves. From this and Eqs. (32) and (37), we have

$$\Phi(\omega)=\frac{\pi\omega}{c(\omega)}\frac{d\rho}{d\omega}\int_0^\infty\overline{\phi}(r)\,J_0\left(\frac{\omega}{c(\omega)}r\right)rdr.$$

Then the Hankel transformation yields the final result:

$$\overline{\phi}(r)=\int_0^\infty \frac{c(\omega)}{\pi\omega}\frac{d\omega}{d\rho}\Phi(\omega)J_0\left(\frac{\omega}{c(\omega)}r\right)\frac{\omega}{c(\omega)}\frac{d\rho}{d\omega}d\omega$$

$$=\frac{1}{\pi}\int_0^\infty \Phi(\omega)J_0\left(\frac{\omega}{c(\omega)}r\right)d\omega \ . \tag{40}$$

6. Spatial autocorrelation of filtered waves (2)

As has been mentioned in Section 3, the measurements in our method are carried out in two steps; first, the seismograph vibrations are filtered, and secondly, among filtered vibrations, the spatial autocorrelation coefficient is computed. So far as we are concerned with waves having a single velocity corresponding to a frequency ω, the azimuthally averaged autocorrelation function $\overline{\phi}(r)$ of the wave filtered by a resonator of frequency ω_0 is written from Eq. (40) as

$$\overline{\phi}(r)\equiv\overline{\phi}(r,\ \omega_0)=P(\omega_0)J_0\left(\frac{\omega_0}{c(\omega_0)}r\right) \tag{41}$$

where $P(\omega_0)$ is the same as defined by Eq. (19). In consequence, denoting the corresponding autocorrelation coefficient $\overline{\rho}(r,\ \omega_0)$, we have

$$\overline{\rho}(r,\ \omega_0)=J_0\left(\frac{\omega_0}{c(\omega_0)}r\right). \tag{42}$$

This formula clearly indicates that if one measures $\overline{\rho}(r,\ \omega_0)$ for a certain r and for various ω_0's, he can obtain the function $c(\omega_0)$, i.e. the dispersion curve of the wave for the corresponding range of frequency ω_0.

Now let us proceed to the cases in which waves are polarized, and later refer to the cases in which they are composed of partial waves having different velocities and the above procedure cannot be applied.

7. Polarization

As far as two dimensional waves propagating over a horizontal plane are concerned, it is evident that there is no polarization with respect to the vertical component of vibrations. On the other hand, the horizontal component has two typical modes of polarization; namely the vibration is confined either in the direction parallel to that of pro-

pagation, or in the direction perpendicular to that. For instance, in the case of seismic waves, P waves, SV waves, and Rayleigh waves belong to the former, while SH waves and Love waves belong to the latter.

In order to deal with those polarized waves, we observe the component vibration u_r parallel to and the other component u_ψ perpendicular to the direction connecting the two seismometers placed, between the vibrations of which the correlation is to be investigated. Denoting spatial autocorrelation functions for these two components as

$$\phi_r(r,\ \psi) \equiv \overline{u_r(x,\ y)u_r(x+r\cos\psi,\ y+r\sin\psi)}$$

$$\phi_\psi(r,\ \psi) \equiv \overline{u_\psi(x,\ y)u_\psi(x+r\cos\psi,\ y+r\sin\psi)}$$

we have from Eq. (31) for waves of the parallel polarization

$$\left.\begin{aligned}\phi_r(r,\ \psi)&=\frac{1}{(2\pi)^2}\iint \cos^2(\theta-\psi)|G(\rho,\ \theta)|^2\exp\{i\rho r\cos(\theta-\psi)\}\rho d\rho d\theta\\ \phi_\psi(r,\ \psi)&=\frac{1}{(2\pi)^2}\iint \sin^2(\theta-\psi)|G(\rho,\ \theta)|^2\exp\{i\rho r\cos(\theta-\psi)\}\rho d\rho d\theta\end{aligned}\right\} \quad (43)$$

and in the same way we have for waves of the perpendicular polarization

$$\left.\begin{aligned}\phi_r(r,\ \psi)&=\frac{1}{(2\pi)^2}\iint \sin^2(\theta-\psi)|G(\rho,\ \theta)|^2\exp\{i\rho r\cos(\theta-\psi)\}\rho d\rho d\theta\\ \phi_\psi(r,\ \psi)&=\frac{1}{(2\pi)^2}\iint \cos^2(\theta-\psi)|G(\rho,\ \theta)|^2\exp\{i\rho r\cos(\theta-\psi)\}\rho d\rho d\theta\end{aligned}\right\}. \quad (44)$$

The above equations show that in both cases the sum of two component autocorrelation functions

$$\phi_r(r,\ \psi)+\phi_\psi(r,\ \psi)$$

is written in the same form as Eq. (31) for non-polarized waves

$$\phi_r(r,\ \psi)+\phi_\psi(r,\ \psi)=\frac{1}{(2\pi)^2}\iint|G(\rho,\ \theta)|^2\exp\{i\rho r\cos(\theta-\psi)\}\rho d\rho d\theta. \quad (45)$$

Thus if we know the left hand side of the above equation, we can obtain, by the use of the Fourier transformation, $|G(\rho,\ \theta)|^2$ which indicates the distribution of direction of wave propagation.

On the other hand, the mode of polarization is shown apparently in the azimuthally averaged autocorrelation functions;

$$\overline{\phi}_r(r)=\frac{1}{2\pi}\int\phi_r(r,\ \psi)d\psi$$

$$\overline{\phi}_\psi(r)=\frac{1}{2\pi}\int\phi_\psi(r,\ \psi)d\psi.$$

From Eq. (43) and the following relations

$$\int_0^{2\pi}\cos^2(\psi-\theta)\exp\{i\rho r\cos(\psi-\theta)\}d\psi=\pi\{J_0(\rho r)-J_2(\rho r)\}$$

$$\int_0^{2\pi}\sin^2(\psi-\theta)\exp\{i\rho r\cos(\psi-\theta)\}d\psi=\pi\{J_0(\rho r)+J_2(\rho r)\}$$

we obtain for the parallel polarization,

$$\left.\begin{aligned}\overline{\phi}_r(r)&=\frac{1}{2}\frac{1}{(2\pi)^2}\iint|G(\rho,\ \theta)|^2\{J_0(\rho r)-J_2(\rho r)\}\rho d\rho d\theta\\ \overline{\phi}_\psi(r)&=\frac{1}{2}\frac{1}{(2\pi)^2}\iint|G(\rho,\ \theta)|^2\{J_0(\rho r)+J_2(\rho r)\}\rho d\rho d\theta\end{aligned}\right\}. \tag{46}$$

In the similar way, we have for the perpendicular polarization,

$$\left.\begin{aligned}\overline{\phi}_r(r)&=\frac{1}{2}\frac{1}{(2\pi)^2}\iint|G(\rho,\ \theta)|^2\{J_0(\rho r)+J_2(\rho r)\}\rho d\rho d\theta\\ \overline{\phi}_\psi(r)&=\frac{1}{2}\frac{1}{(2\pi)^2}\iint|G(\rho,\ \theta)|^2\{J_0(\rho r)-J_2(\rho r)\}\rho d\rho d\theta\end{aligned}\right\}. \tag{47}$$

If the correlation is taken among the vibrations filtered by a resonator of frequency ω_0, we may write

$$\frac{1}{2\pi}\int|G(\rho,\ \theta)|^2\rho d\theta=P(\omega_0)\delta\left(\rho-\frac{\omega_0}{c(\omega_0)}\right). \tag{48}$$

Then inserting this into Eq. (46), we have the corresponding azimuthally averaged autocorrelation functions for the parallel polarization,

$$\left.\begin{aligned}\overline{\phi}_r(r,\ \omega_0)&=\frac{1}{2}P(\omega_0)\left\{J_0\left(\frac{\omega_0}{c(\omega_0)}r\right)-J_2\left(\frac{\omega_0}{c(\omega_0)}r\right)\right\}\\ \overline{\phi}_\psi(r,\ \omega_0)&=\frac{1}{2}P(\omega_0)\left\{J_0\left(\frac{\omega_0}{c(\omega_0)}r\right)+J_2\left(\frac{\omega_0}{c(\omega_0)}r\right)\right\}\end{aligned}\right\}. \tag{49}$$

Likewise we have for the perpendicular polarization,

$$\left.\begin{aligned}\overline{\phi_r}(r,\ \omega_0)&=\frac{1}{2}P(\omega_0)\left\{J_0\left(\frac{\omega_0}{c(\omega_0)}r\right)+J_2\left(\frac{\omega_0}{c(\omega_0)}r\right)\right\}\\ \overline{\phi_\psi}(r,\ \omega_0)&=\frac{1}{2}P(\omega_0)\left\{J_0\left(\frac{\omega_0}{c(\omega_0)}r\right)-J_2\left(\frac{\omega_0}{c(\omega_0)}r\right)\right\}\end{aligned}\right\}. \tag{50}$$

From the above formulas it is clear that the measurement of $\overline{\phi_r}(r,\ \omega_0)$ and $\overline{\phi_\psi}(r,\ \omega_0)$ will effectively determine the polarization of the wave.

8. Special cases

In this section we shall consider the following two special cases; (a) $|G(\rho,\ \theta)|^2$ is independent of θ, (b) $|G(\rho,\ \theta)|^2$ is zero except for $\theta=\theta_0$ and $\theta=\theta_0+\pi$. For instance, the case of microtremors will be shown in Chapter 3 to be of the former type, while seismic waves due to earthquakes may belong to the latter if observed at a point distant from their origin. We shall call the former wave an "isotropic wave" and the latter a "plane wave".

In the case of the isotropic wave, writing

$$|G(\rho,\ \theta)|^2\equiv|G(\rho)|^2\,, \tag{51}$$

we get from Eq. (31)

$$\phi(r,\ \psi)=\frac{1}{2\pi}\int_0^\infty|G(\rho)|^2J_0(\rho r)\rho d\rho\ . \tag{52}$$

Thus $\phi(r,\ \psi)$ is independent of ψ, and it is clear that in this case we can replace $\overline{\phi}(r)$ by $\phi(r,\ \psi)$ for an arbitrary ψ in the formulas obtained previously, and we need not take the average of $\phi(r,\ \psi)$ with respect to ψ. This also holds for polarized isotropic waves.

On the other hand, in the case of the plane wave, we may write

$$|G(\rho,\ \theta)|^2=|G'(\rho)|^2\delta(\theta-\theta_0) \tag{53}$$

and we have

$$\phi(r,\ \psi)=\frac{1}{2\pi}\int|G'(\rho)|^2\cos\{\rho r\cos(\psi-\theta_0)\}\rho d\rho\ . \tag{54}$$

If we observe the wave filtered by a resonator of frequency ω_0, it follows from Eqs. (48) and (53) that

$$\frac{1}{2\pi}\int|G(\rho,\ \theta)|^2\rho d\theta=|G'(\rho)|^2\rho=P(\omega_0)\delta\left(\rho-\frac{\omega_0}{c(\omega_0)}\right)\ . \tag{55}$$

Then the corresponding autocorrelation function $\phi(r,\ \psi,\ \omega_0)$ is written as

$$\phi(r,\ \psi,\ \omega_0)=P(\omega_0)\cos\left\{\frac{\omega_0}{c(\omega_0)}r\cos(\psi-\theta_0)\right\} \tag{56}$$

and also the corresponding autocorrelation coefficient as

$$\rho(r,\ \psi,\ \omega_0)\equiv\frac{\phi(r,\ \psi,\ \omega_0)}{\phi(0,\ \psi,\ \omega_0)}=\cos\left\{\frac{\omega_0}{c(\omega_0)}r\cos(\psi-\theta_0)\right\} \tag{57}$$

or

$$\frac{\cos(\psi-\theta_0)}{c(\omega_0)}=\frac{1}{r\omega_0}\{(-1)^n\operatorname{Cos}^{-1}\rho(r,\ \psi,\ \omega_0)+n\pi\}\ . \tag{58}$$

This last formula (58) shows that we can determine the velocity $c(\omega_0)$ and the angle θ_0 of the direction of propagation by measuring $\rho(r,\ \psi,\ \omega_0)$ at two different ψ's, provided the value of n is known beforehand.

Likewise, in the case of polarized plane wave, we have, for instance, for the parallel polarization

$$\left.\begin{aligned}\phi_r(r,\ \psi,\ \omega_0)&=\cos^2(\theta_0-\psi)P(\omega_0)\cos\left\{\frac{\omega_0}{c(\omega_0)}r\cos(\psi-\theta_0)\right\}\\ \phi_\psi(r,\ \psi,\ \omega_0)&=\sin^2(\theta_0-\psi)P(\omega_0)\cos\left\{\frac{\omega_0}{c(\omega_0)}r\cos(\psi-\theta_0)\right\}\end{aligned}\right\}. \tag{59}$$

In this case, although the velocity and the direction of propagation can still be known after the normalization which is needed to obtain the corresponding autocorrelation coefficient, the mode of polarization cannot be. Therefore, the polarization for an ideal plane wave is better determined by the ordinary method by investigating the amplitudes for various azimuthal angles.

Our method will, however, be effectively applied to a wave composed of two independent waves, which differ from each other in the

mode of polarization and in the velocity of propagation. The general nature of the plane stochastic waves will be given elsewhere in the future in connection with seismic waves.

9. Velocity distribution

In this section we shall deal with two dimensional waves of multiple velocities. Supposing that our waves are not polarized, and denoting a quantity related to the n'th component wave by attaching the suffix n, we write our wave in the form,

$$u=\sum_n u_n(x, y, t) .$$

Assuming the statistical independence among the component waves as in the case of one dimensional waves we get the following relations,

$$\begin{aligned}
\phi(r, \psi)&=\sum_n \phi_n(r, \psi)\\
\overline{\phi}(r)&=\sum_n \overline{\phi}_n(r)\\
\overline{\phi}(r, \omega_0)&=\sum_n \overline{\phi}_n(r, \omega_0)=\sum_n P_n(\omega_0)J_0\left(\frac{\omega_0}{c_n(\omega_0)}r\right)\\
\overline{\rho}(r, \omega_0)&=\sum_n \frac{P_n(\omega_0)}{P(\omega_0)}J_0\left(\frac{\omega_0}{c_n(\omega_0)}r\right) .
\end{aligned} \tag{60}$$

This last equation (60) indicates that if the number N of component waves is finite, we can obtain the velocity and the percentage of power for each component by measuring $\overline{\rho}(r, \omega_0)$ for a given ω_0 and for $(2N-1)$ different r's.

It may happen, as in the case of one dimensional waves, that the velocity of component waves is distributed continuously. For such a wave group, we define the velocity distribution function by the relation,

$$p(\omega_0, c_n)\Delta c_n=P_n(\omega_0) ,$$

and then we can write

$$\overline{\phi}(r, \omega_0)=\int p(\omega_0, c)J_0\left(\frac{\omega_0}{c(\omega_0)}r\right)dc . \tag{61}$$

From this it follows by the use of the Hankel transformation that

$$\frac{p(\omega_0,\ c)}{P(\omega_0)}=\frac{\omega_0}{c^3}\int_0^\infty \bar{\rho}(r,\ \omega_0)J_0\left(\frac{\omega_0}{c(\omega_0)}r\right)rdr\ . \tag{62}$$

Thus we have the formula by which to determine the velocity distribution function from the value of $\bar{\rho}(r,\ \omega_0)$ for $r=0\sim\infty$ in the case of two dimensional waves. Eq. (62) corresponds to Eq. (24) for one dimensional waves.

In the case of the polarized wave of multiple velocities, we see from the results obtained in Section 7, that if we replace, for instance, $\overline{\phi}(r,\ \omega_0)$ by the sum of the component autocorrelation functions,

$$\overline{\phi}_r(r,\ \omega_0)+\overline{\phi}_\psi(r,\ \omega_0)$$

every formula in this section holds unaltered.

10. Discussions and summary

The results obtained in the preceding sections indicate that the study of waves from the viewpoint of spectrum will give us additional informations which have been neglected because of the lack of proper method of analysis for the purpose. We have dealt with one dimensional stochastic waves in detail, and extended the reasoning followed there to two dimensional waves. It will be easy to proceed to the investigation of three dimensional waves, but this does not seem to be practically necessary for our measurements of waves are usually confined on a plane surface.

We shall enumerate here the principal results obtained in the present chapter.

(1) The spatial autocorrelation coefficient $\rho(\xi,\ \omega_0)$ of a one dimensional wave having a single velocity c and being filtered by a resonator of frequency ω_0 is given by the relation,

$$\rho(\xi,\ \omega_0)=\cos\left(\frac{\omega_0}{c}\xi\right)\ . \tag{21}$$

This holds also for a dispersive wave with the substitution of $c(\omega_0)$ for the constant velocity c.

(2) If we are allowed to assume a continuous distribution of velocity in a stochastic one dimensional wave, we can obtain the velocity distribution function $p(\omega_0,\ c)$ in the form,

$$\frac{p(\omega_0,\ c)}{P(\omega_0)}=\frac{2}{\pi c^2}\int_0^\infty \rho(\xi,\ \omega_0)\cos\left\{\frac{\omega_0}{c(\omega_0)}\xi\right\}d\xi\,. \tag{24}$$

(3) In the case of a two dimensional wave having a single velocity and being not polarized, a one to one correspondence is found between the azimuthally averaged spatial autocorrelation function

$$\bar{\phi}(r)=\frac{1}{2\pi}\int_0^{2\pi}\phi(r,\ \psi)d\psi$$

and the spectrum density $\Phi(\omega)$ in time as follows,

$$\Phi(\omega)=\frac{\pi\omega}{c^2}\int_0^\infty \bar{\phi}(r)J_0\left(\frac{\omega}{c}r\right)rdr\,, \tag{38}$$

$$\bar{\phi}(r)=\frac{1}{\pi}\int_0^\infty \Phi(\omega)J_0\left(\frac{\omega}{c}r\right)d\omega\,. \tag{39}$$

(4) The azimuthally averaged spatial autocorrelation coefficient of the above wave being filtered by a resonator of frequency ω_0 is given by the relation,

$$\bar{\rho}(r,\ \omega_0)=J_0\left(\frac{\omega_0}{c}r\right)\,. \tag{42}$$

This holds also for a dispersive wave of two dimensions with the substitution of $c(\omega_0)$ for constant c.

(5) In the case of a polarized wave, we observe two component autocorrelation functions; namely, an azimuthal component ϕ_ψ and a radial one ϕ_r. It was shown that the sum of these components behaves in the same way as the autocorrelation function of a non polarized wave does. The azimuthal averages of these two ϕ's for the wave filtered by a resonator of frequency ω_0, reflect its mode of polarization and are written in the form,

$$\left.\begin{aligned}\bar{\phi}_r(r,\ \omega_0)&=\frac{1}{2}P(\omega_0)\left\{J_0\left(\frac{\omega_0}{c(\omega_0)}r\right)-J_2\left(\frac{\omega_0}{c(\omega_0)}r\right)\right\}\,,\\ \bar{\phi}_\psi(r,\ \omega_0)&=\frac{1}{2}P(\omega_0)\left\{J_0\left(\frac{\omega_0}{c(\omega_0)}r\right)+J_2\left(\frac{\omega_0}{c(\omega_0)}r\right)\right\}\,,\end{aligned}\right\} \tag{49}$$

for the parallel polarization. These for the perpendicular polarization are written as

$$\left.\begin{aligned}\overline{\phi}_r(r,\omega_0)&=\frac{1}{2}P(\omega_0)\left\{J_0\left(\frac{\omega_0}{c(\omega_0)}r\right)+J_2\left(\frac{\omega_0}{c(\omega_0)}r\right)\right\},\\ \overline{\phi}_\psi(r,\omega_0)&=\frac{1}{2}P(\omega_0)\left\{J_0\left(\frac{\omega_0}{c(\omega_0)}r\right)-J_2\left(\frac{\omega_0}{c(\omega_0)}r\right)\right\}.\end{aligned}\right\} \tag{50}$$

(6) The velocity distribution function for a two dimensional wave is written in the form,

$$\frac{p(\omega_0,\ c)}{P(\omega_0)}=\frac{\omega_0}{c^3}\int_0^\infty\overline{\rho}(r,\ \omega_0)J_0\left(\frac{\omega_0}{c(\omega_0)}r\right)rdr\,. \tag{62}$$

Chapter 2. Apparatus

Theoretical considerations in Chapter 1 have shown that the spatial autocorrelation coefficient of the filtered waves plays an important role in the spectral study of stationary stochastic waves. In order to obtain the value of the coefficients with respect to a given wave, it is necessary first to filter the vibration of every seismometer by a resonator having a certain assigned frequency, and secondly to compute the correlation coefficient for every pair of the filtered vibrations. Fig. 1 is the block diagram of an assembly of apparatus corresponding to one pair of seismometers.

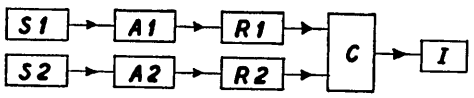

Fig. 1. Block diagram of apparatus.

S; seismometer
A; amplifier
R; resonator
C; correlation computer
I; indicator

In the study of waves from the viewpoint of "phases", the recording of vibration is essential for identifying the phases and for reading travel times. In our method, on the other hand, what we need is not the original record, but the result of the above described operations applied to them. Those operations may be carried out manually, but it should be emphasized that the troublesome labours involved in the manual operations make the application of our method practically impossible. The present study has been made possible by the automation of the operations. In fact, the theoretical studies given in Chapter 1 were initiated after the completion of a correlation computer in our laboratory, though the use of filters in our method was based on the theoretical results.

Of the elements constituting our apparatus shown in Fig. 1, seismo-

meters and amplifiers are the ordinary ones, and we need not give any detailed explanation about them. We shall describe in this chapter the details of our filter and correlation computer.

1. Filter of phase shift type

This type of resonator is rather well known in Electronics. The fundamental part of this circuit is shown in Fig. 2. If the resistance r_1 is equal to r_2, the ratio of the amplitude of output voltage to that of input voltage becomes 1/2 independent of the frequency of the input, while the phase angle shifted by the circuit depends on the frequency. This dependence is as follows; the phase angle shifted for the zero frequency is π, that for the infinite frequency is 0, while that for the frequency $f_0=1/2\pi RC$ is $\pi/2$. Therefore, if two such circuits are connected in series, the resultant phase angle shift will be nearly zero for the whole range of frequency except for the neighbourhood of $f_0=1/2\pi RC$, where the corresponding angle is nearly equal to π. Putting the resultant output into a phase inverter and putting the output of the inverter to the control grid of the first valve of the phase shift circuit result in a positive feedback for the neighbourhood of the frequency f_0 and a negative one for the else. Thus the circuit as a whole works as a resonator of frequency f_0.

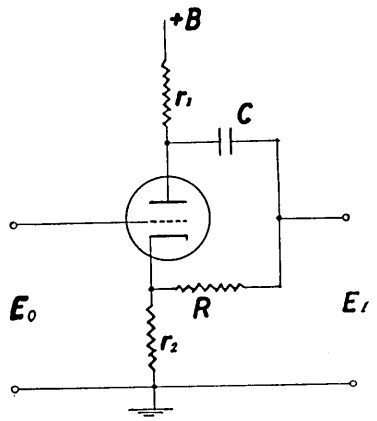

Fig. 2. Circuit for phase shift.

For the purpose of the present study we need at least two resonators having the same characteristics, and moreover their resonance frequency should cover a considerable range which depends on the nature of waves to be studied. Since microtremors due to traffic will be the first object of our study, the resonators were designed to have a frequency range covering continuously from 5 c/s to 30 c/s. The variation of resonance frequency in the resonator was made by the use of variable resistances in the phase shift circuit.

A filter of this type is much easier to construct than a filter having inductances, but the Q value attainable is rather low. In our case, stable operation for a long time was not possible at a value of Q higher

than 30.

At the time of observation, we must adjust the characteristics of the two filters in order that the resonance frequencies and Q values of both will be equal. For this purpose we are using a standard oscillator and an oscilloscope as shown in Fig. 3. At first the frequency of one of the filters is adjusted to be equal to an assigned frequency of the standard oscillator by the aid of the Lissajous' figure on the oscilloscope, and then the frequency of the other filter is adjusted to be equal to the assigned frequency in the same way. The Q value of our filter depends on the feedback constant which is controled by a variable resistance. In order to equalize the Q values of the two filters, we connect the output of one of the filters to the horizontal input of the oscilloscope and that of the other to the vertical one, and observe the response figure caused by the simultaneous application of an impulse to both filters. If the response figure on the oscilloscope diminishes in size keeping a similar shape, we regard that the adjustment is finished.

2. Automatic computer of the correlation coefficient

A computer for calculating the correlation coefficient according to the ordinary way needs the following parts; an input device such as tape or card system, arithmetic elements to make additions and multiplications, and an output device such as a printing machine or some other indicators. So far as we stick to this customary method of computation, the computing machine will become a large one, which cannot be very inexpensive. But if we use the simplified method proposed by Tomoda[3] (1956), the computer will become a very simple one.

In the method due to Tomoda, the original stochastic variable is replaced by $+1$ when it is above the mean value, and by -1 when it is below the mean value. Then the computation of the correlation coefficient in the ordinary way is applied to the resultant series of $+1$ and -1. If this value obtained is r, the true correlation coefficient ρ is deduced by the following formula,

$$\rho=\sin\frac{\pi}{2}r\ .$$

Since the mean value of the deflection of a seimometer pendulum can

3) Y. TOMODA, *Jour. Phys. Earth*, **4** (1956), 67.

be assumed as zero, we can write the above r in the form,

$$r=\frac{n_+-n_-}{n_++n_-}$$

where n_+ is the number of sample pairs for which the deflection of one of the seismometers has the same sign as that of the other, while n_- is the number of sample pairs for which their signs are opposite.

This simplified method was applied to seismograms in a correlogram analysis by Aki[4] (1956) which proved its effectiveness. Akamatu[5] (1956) compared the correlogram of a given time series obtained by this method with that obtained by the customary method, and showed that the agreement between them is satisfactory, as the wave form of the given time series is not very complicated. The application of this simplified method in the present case is justified because the computation is actually made with regard to the filtered vibration having an almost sinusoidal wave form.

The parts of our computer are as follows; a generator of pulses, circuits to compare the sign of the signal coming from one of the seismometers with that from the other, and decatron which works as a counting tube as well as an indicator.

At first we shall describe how to count the number of sample pairs for which the signal from the seismometer S_1 and that from S_2 both have the positive sign. Pulses from a generator, which is a one shot multivibrator triggered by a thyratron oscillator, play the part of sampling in the following way. If we use a frequency converting valve, e.g. 6*SA*7, having two control grids, of which one is fed by the series of pulses coming from the generator and the other by the signal coming from the seismometer S_1 as shown in Fig. 5, the output is a series of pulses as shown in Fig. 4-*c*. The height of each pulse is now proportional to the height of the signal from S_1, when the latter has the positive sign. When it is negative, no output pulses will appear. Therefore putting this series of output pulses into another one shot multivibrator, we obtain the series of pulses which appear only when the signal from S_1 has the positive sign. These pulses are now of the same height as shown in Fig. 4-*d*. Finally, if the same operation is applied to the above pulses and the signal S_2 as is done to the pulses from the generator and the signal from S_1, we have the series of pulses

4) K. AKI, *Jour. Phys. Earth*, **4** (1956), 71.
5) K. AKAMATU, *ibid.*, 81.

which appear only when both the signals from S_1 and from S_2 have the positive sign as shown in Figs. 4-*e*, 4-*f* and 4-*g*.

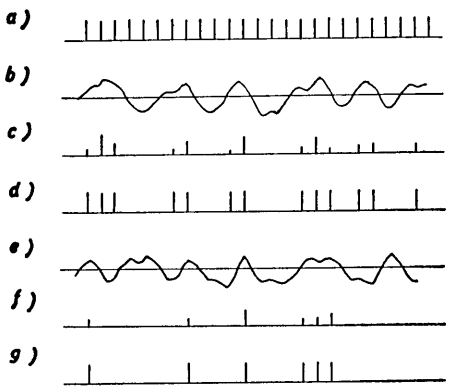

Fig. 4. Process of computation shown schematically,
a) pulses from a pulse generator,
b) signal from the seismometer 1,
c) and *d*) pulses which exist when the signal from *S*1 is positive,
e) signal from the seismometer 2,
f) and *g*) pulses which exist when the signals from both seismometers are both positive.

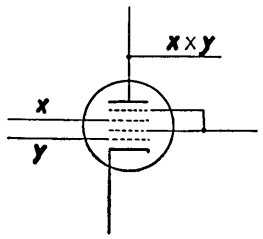

Fig. 5. 6*SA*7 as a multiplier.

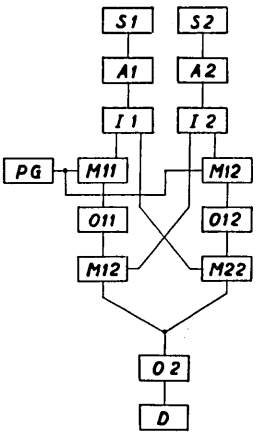

Fig. 6. Block diagram of computer.
S; seismometer
A; amplifier
I; phase inverter
M; multiplier
PG; pulse generator
O; one-shot multi-vibrator
D; decatrons

The series of pulses which appear when both of them have the negative sign will be generated in the same way as above except for the use of phase inverters applied beforehand to the signals from both seismometers. The two series of pulses thus obtained are counted in a decatron circuit, and the number n_+ of the sample pairs for which the signs of the signals from both seismometers are the same is obtained. Since we are using three decatrons in series, we can count up to one thousand. The processes above described may be understood by the block diagram in Fig. 6.

The counting of n_- is carried out in the same way as that of n_+ but with the reverse connection of the outputs of one of the inverters.

The result of counting is indicated on the decatrons. Photographs

of our computer and the decatron indicator are shown in Fig. 7 and Fig. 8.

3. Remarks

The choice of the time interval of successive pulses from the generator depends on the nature of waves to be studied. Since our primary object was microtremors of traffic origin, the time interval was taken as 1/50 second considering that the predominant period of the tremors is 1/10 second. Of course, not only the pulse interval but also the frequency range of the resonator and the characteristics of the seismometers should be appropriate to the spectral nature of the waves concerned. The whole apparatus designed for microtremors will be applied without modifications to volcanic tremors or to ground motions having rather high frequencies caused by some meteorological disturbances. On the other hand, in order to investigate waves having lower frequencies, we need some modifications of the apparatus.

As far as we are concerned with almost perfectly stationary waves, that is waves having sufficiently long durations that we can, not only obtain the correlation coefficients from large samples, but also repeat the measurement several times under the same circumstances, we need only one set of apparatus, i.e. a pair of seismometers, a pair of filters, and one correlation computer. There is, however, another important class of waves having intermediate durations, which are long enough for the computation of correlation coefficient, but nevertheless are too short for repeated measurements. To this class of waves belong some parts of the seismic waves of earthquake origin. The measurement of this latter kind of waves will be very difficult without the use of storage units such as magnetic tapes or magnetic discs.

We shall note some features of the apparatus which seem peculiar to the present method. Since a very sharp filtration is applied to the vibration, troubles with the noises in the amplifier such as caused by the hum in the power source are considerably diminished. In addition, since the correlation between the simultaneous vibrations at two points is under question, the uneven phase lag and amplification as to the frequency on the part of the seismometer and the amplifier cannot be serious matters, for the pair of seismometers and also of amplifiers are made to have identical characteristics.

Chapter 3. Microtremors

In this chapter, our method described in the preceding chapters will be applied to microtremor analyses. The microtremor studied for this purpose is believed to be caused by traffic and appears as an undesirable background noise in many precise geophysical measurements. The choice of this as our object is partly due to the handiness of its measurement as a trial application of our method but also due to the fact that the microtremor itself has formed one of the important problems in Seismology, especially in Japan.

It is well known that the characteristics of the ground are reflected more or less in its vibration whatever the origin of the vibration may be. This fact was noticed early in the beginning of this century by K. Sekiya and F. Omori who made a comparative study of seismograms recorded at Hongo and Hitotsubashi, both in Tokyo. Later, many Japanese seismologists studied ground vibrations from the view point of frequency spectrum. Among them, M. Ishimoto[6] (1937) made a systematic study both of vibrations due to earthquakes and of the background tremors, and proposed a hypothesis that the predominant period of vibration due to earthquakes coincides with that of the background tremors.

Though some negative results against the above hypothesis have been obtained by P. Byerly[7] (1947) and by K. Aki[8] (1955), the spectral study of the background tremors was succeeded in by various authors.

Y. Tomoda and K. Aki[9] (1952) made a frequency analysis by the use of a spectrometer, and confirmed the fact that vibrations having frequencies higher than 1 c/s are due to traffic. K. Kanai, T. Tanaka and K. Osada[10] (1954) made an extensive study and showed that the form of the spectral distribution of microtremors coincides with that of earthquake motions, and that it depends on the geology of the place. K. Akamatu[11] (1956) investigated the tremors observed at Hongo in more detail from the view point of correlograms in space and time.

6) M. ISHIMOTO, *Bull. Earthq. Res. Inst.*, **15** (1937), 697.
7) P. BYERLY, *Bull. Seis. Soc. Amer.*, **37** (1947), 291.
8) K. AKI, *Zisin*, [ii], **8** (1955), 99.
9) Y. TOMODA and K. AKI, *Zisin*, [ii], **5** (1952).
10) K. KANAI, T. TANAKA and K. OSADA, *Bull. Earthq. Res. Inst.*, **32** (1954), 199.
11) K. AKAMATU, *Zisin*, [ii], **9** (1956), 21.

Ishimoto's hypothesis implies a resonance phenomenon in the surface layer, and this problem has been attacked theoretically by various authors. In the following section, we shall refer to some of them assuming the hypothetical wave type of the microtremors.

1. Preliminary discussions

It will be useful to make a preliminary consideration about the wave type of the microtremors. It may be assumed that the type is one of the following four.

A. A surface wave in a narrow sense; this terminology is due to Y. Sato[12] (1954), and represents the wave having an apparent velocity along the horizontal surface which is determined if the frequency is given. If we apply our method to the wave of this type, we can obtain a definite velocity corresponding to a given frequency of the resonator by which the vibrations are filtered. And the autocorrelation function will take the form of Eq. (41), Eq. (49), or Eq. (50).

B. The vibration of a soft surface layer due to a vertically incident bodily wave such as that dealt with by R. Takahasi and K. Hirano[13] (1941); it was shown in their paper that the vibration of this type shows predominant amplitudes at the frequencies, $f=V/4H$, $3V/4H$, $5V/4H$, etc., where V is the velocity of bodily wave in the layer and H is the thickness of the layer. It will be expected in this case that the spatial autocorrelation coefficient with respect to the vibration filtered by a resonator having the predominant frequency, becomes independent of the distance r and is equal to unity.

C. The vibration of a surface layer due to an obliquely incident bodily wave which was studied for instance by G. Nishimura and T. Takayama[14] (1939); a kind of resonance phenomena is observed in this case. We assume that the microtremor belongs to this type, and consists of various vibrations resulting from waves of different incident angles. The vibration of this type is evidently not the surface wave in the narrow sense difined by Y. Sato, because the apparent velocity of this wave along the surface cannot be definite even if the frequency is given. If our method is applied to the wave of this type, a continuous distribution of velocity, that is described in Sections 3 and 9 of Chapter

12) Y. SATO, *Bull. Earthq. Res. Inst.*, **32** (1954), 161.

13) R. TAKAHASI and K. HIRANO, *Bull. Earthq. Res. Inst.*, **19** (1941), 534.

14) G. NISHIMURA and K. TAKAYAMA, *Bull. Earthq. Res. Inst.*, **17** (1939), 253, 308, 319.

1, will be observed instead of definite velocities.

D. The vibration due to a periodically distributed surface disturbance such as that illustrated in the paper of K. Sezawa and K. Kanai[15] (1937); it was shown that a resonance phenomenon occurs when the frequency of vibration is equal to the solution of the characteristic equation of a surface wave for the wave length which is equal to that of the distribution of given disturbance. In this case, the form of spatial autocorrelation coefficients with respect to the vibrations filtered by resonators of various frequencies will be independent of the frequency, and will be determined by the spatial pattern of the given distrubance.

Bearing the above four types in mind and applying our correlational analyses to the microtremor at Hongo, in Tokyo, we shall be able to determine its wave type together with its several important characteristics.

2. Microtremors at Hongo

The measurement was made in the yard of the Geophysical Institute of Tokyo University, of which a map is shown in Fig. 9. In this map are shown the lines along which the spatial autocorrelation is obtained, three wooden buildings by thin line rectangles and an abandoned tennis court by a dotted line rectangle. This is the same place where K. Akamatu (1956) studied the spectrum of prevailing microtremors. The predominant frequencies of the tremors were found by her to lie at $3 \sim 4$ c/s and at $7 \sim 10$ c/s. In the present study, we shall deal with the vibrations having frequencies higher than 5 c/s, leaving the vibrations having lower frequencies including $3 \sim 4$ c/s to a later study.

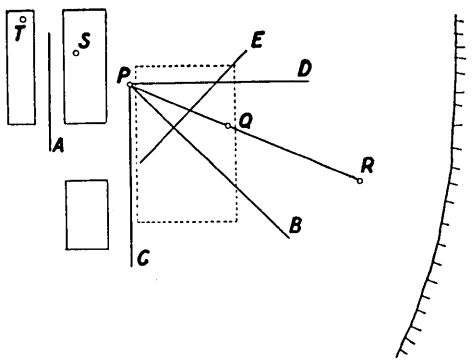

Fig. 9. Map showing lines of measurement.

Seismometers used in the present investigation are all of the moving coil type; a pair of horizontal ones having the free frequency of 10 c/s, a pair of horizontal ones of the frequency of 4.5 c/s, and a pair of vertical ones of the frequency of 4.5 c/s.

15) K. SEZAWA and K. KANAI, *Bull, Earthq. Res. Inst.*, **14** (1938), 1.

The observation of the tremors was usually made during the night time from 18h to 22h, because the daytime observation is disturbed severely by the noise due to persons walking in and around the place.

At the time of measurement, one of the pairs of seismometers is set up along the line of measurement, and the signals coming from them are sent through wires to the amplifiers placed in the laboratory to be analysed by the resonators and the correlation computer. The correlation coefficient obtained from the sampling during a short period varies notably with time, for instance, 50 second sampling yields the correlation coefficient, for a seismometer pair 20 meters apart from each other, varying from 0.5 to -0.9. Therefore a sampling time of at least five or ten minutes is needed, this corresponding to the sample size of more than five thousands.

3. Direction of propagation

Fig. 10 shows the autocorrelation coefficients measured along the lines *B*, *C*, *D*, and *E* in Fig. 9. In this measurement, horizontal seismometers having the frequency of 10 c/s are used and filtration is not applied. Since the curves in the figure differ only slightly from one another, we may regard the microtremor as being propagated in every direction, each with almost uniform power. Thus it may be allowed to replace the azimuthally averaged autocorrelation function by the autocorrelation function taken along any line having an arbitrary azimuthal angle. (See Section 8, Chapter 1.)

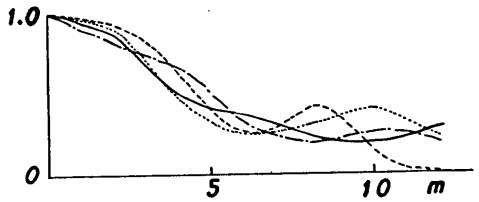

Fig. 10. Autocorrelation coefficients for various directions.

4. Horizontal heterogeneity

It was found, however, that the autocorrelation coefficient taken along a segment of a line sometimes differs significantly from that taken along another segment of the same line. An example is shown in Fig. 11, where the dotted curve represents the autocorrelation coefficient taken along the line segment *PQ*, and the other curve shows that taken along *QR*. In both cases, the horizontal seismometers are set up in such a direction as to be sensitive to the vibration which is perpendi-

cular to the line, and the signals from them are filtered by resonators of frequency 9.0 c/s. This fact evidently shows that the wave in question is not stationary in space and can not be adequately dealt with by the present method. We can, however, partly get rid of this difficulty by dealing with the wave within smaller confined areas individually. This may be justified by the fact that the above heterogeneity is due to the existence of the abandoned tennis court convered by a hard surface soil. The fatal difficulty was caused by this heterogeneity in the reduction of the velocity distribution function which was introduced in Sections 3 and 9, Chapter 1, because for its reduction the values of correlation coefficient between two seismometers reasonably apart from each other is needed.

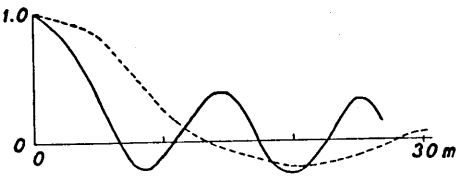

Fig. 11. Comparison of autocorrelatio coefficients measured along the lines PQ and QR.

Under this circumstance the distinction between the type A and C mentioned in Section 1 may fail to be drawn clearly. We may, however, identify the type of our wave as A, if a wave having a single and definite velocity is predominant in the wave and the obtained correlogram has a simple form.

5. Horizontal motions

Before presenting the result of measurements, we shall look back at the theoretical considerations given in Chapter 1. If a certain type of polarized wave is predominant in microtremors, the autocorrelation function with respect to the wave filtered by a resonator of frequency ω_0 will be given either in the form (49) or in the form (50), depending on the mode of polarization. Since we can assume that both $\phi_r(0, \psi)$ and $\phi_\psi(0, \psi)$ are independent of the azimuthal angle ψ in this case, we have the following autocorrelation coefficients for the parallel polarization,

$$\left.\begin{aligned}\rho_r(r, \omega_0) &= J_0\left(\frac{\omega_0}{c(\omega_0)}r\right) - J_2\left(\frac{\omega_0}{c(\omega_0)}r\right)\\ \rho_\psi(r, \omega_0) &= J_0\left(\frac{\omega_0}{c(\omega_0)}r\right) + J_2\left(\frac{\omega_0}{c(\omega_0)}r\right),\end{aligned}\right\} \tag{63}$$

while for the perpendicular polarization,

$$\left.\begin{aligned}\rho_r(r,\ \omega_0)&=J_0\left(\frac{\omega_0}{c(\omega_0)}r\right)+J_2\left(\frac{\omega_0}{c(\omega_0)}r\right)\\ \rho_\psi(r,\ \omega_0)&=J_0\left(\frac{\omega_0}{c(\omega_0)}r\right)-J_2\left(\frac{\omega_0}{c(\omega_0)}r\right),\end{aligned}\right\} \tag{64}$$

where $\rho_r(r,\ \omega_0)$ and $\rho_\psi(r,\ \omega_0)$ are the autocorrelation coefficients for the azimuthal and radial components of vibrations respectively. In Fig. 12 the curves $J_0(x)-J_2(x)$ and $J_0(x)+J_2(x)$ are plotted. With the aid of a table of Bessel functions, the arguments giving the zero, maximum and minimum values of the above curves together with the values of the maxima and minima can be obtained as given in Table I.

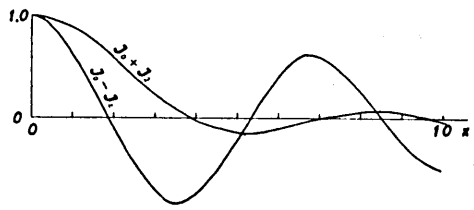

Fig. 12. Curves of $J_0(x)+J_2(x)$ and $J_0(x)-J_2(x)$.

First will be given the result of measurements along the line segment QR in the map in Fig. 9.

Table I. Arguments giving the zeros, maxima and minima.

	x	$J_0(x)-J_2(x)$	x	$J_0(x)+J_2(x)$
1st zero	1.85	0	3.9	0
1st min.	3.50	−0.85	5.1	−0.14
2nd zero	5.35	0	7.0	0
1st max.	6.75	0.62	8.5	0.07
3rd zero	8.55	0	10.0	0
2nd min.	10.1	−0.5		
4th zero	11.7	0		

The azimuthal component of autocorrelation coefficient of the horizontal motion of frequency 9 c/s along this line segment is already given by a full line curve in Fig. 11 in the preceding section. This curve resembles as a whole $J_0(x)-J_2(x)$ in Fig. 12 in form, and the values of the maxima and minima for these two are almost equal except for a notable difference in the 1st minimum value. Since the correlation coefficient is obtained in such a way that one of the pair of seismometers is fixed at the point Q, while the other is moved along QR, this difference may be attributed to the effect of the hard surface soil of the tennis court shown in Fig. 9.

If we measure the correlation coefficient for various frequencies ω_0

and for a fixed distance r, we have the result as shown in Fig. 13, where the distance is 25 meters, and the direction of vibration is perpendicular to QR. This measurement was repeated three times, each on different days but at almost the same hour. Fig. 13 shows that the autocorrelation curve is well reproducible. Also it can be seen that the first maximum of the curve appears at the frequency of 6.4 c/s, and the maximum value amounts to 0.66 which is almost equal to the corresponding value of $J_0(x)-J_2(x)$.

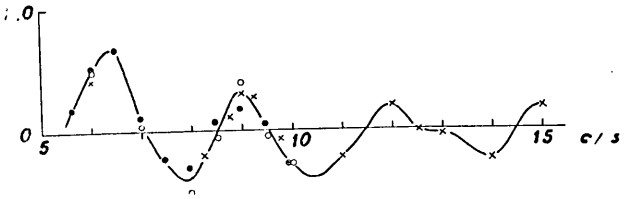

Fig. 13. $\rho(\omega_0, r)$, for $r=25$ m, plotted against ω_0.

These facts suggest that we may assume that the predominant wave in the horizontal motion of microtremor is the one having a single definite velocity and being polarized in the direction perpendicular to that of propagation. Then we can obtain the velocities for various frequencies by identifying the zeros, maxima and minima of the curve in Fig. 13 with those given in Table I. For instance, we have the following equation corresponding to the first maximum,

$$2\pi \cdot 6.4(\mathrm{c/s}) \cdot \frac{25(\mathrm{m})}{C_{6.4}} = 6.75 \ .$$

Thus the wave velocity for the frequency 6.4 c/s is obtained as 148 m/s. The velocities for various frequencies are plotted in Fig. 17 by the mark ○.

A similar measurement is made for the seismometer pair 15 m apart from each other. The resultant autocorrelation coefficient is plotted against the frequency of resonators in Fig. 14. The wave velocities are obtained from this curve in the same way as stated in the preceding paragraph, and are plotted also in Fig. 17 by the mark ●. A good coincidence is observed between the velocity values obtained from two independent measurements as shown in Fig. 17.

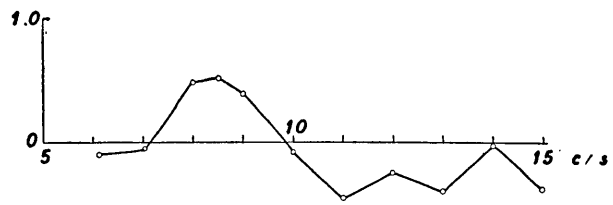

Fig. 14. $\rho(\omega_0, r)$, for $r=15$ m, plotted against ω_0.

Fig. 15 shows the result of a similar measurement in which the distance between the seismometers is 7.5 m. Since in this case the seismometers are placed too near the tennis court covered by hard surface soil, the departure of the autocorrelation curve from the theoretical one, $J_0(x)-J_2(x)$, is considerable, and the velocities cannot be deduced.

A similar measurement is also made about the radial component of the autocorrelation coefficient of the horizontal motion, and the result is shown in Fig. 16 by a full line, where the distance between two seismometers is 25 m. It is confirmed, by observing correlations for a fixed frequency and various distances, that the maximum which appears in Fig. 16 at the frequency of about 7.3 c/s is the first maximum. Therefore the extrapolation of the curve toward lower frequencies as in Fig. 16 is justified at least as a general trend. It is clear from the figure that the value of the first maximum is very small compared with that for the azimuthal component which is shown by a dotted line, and slightly larger than that of $J_0(x)+J_2(x)$ which is theoretically expected. Moreover, the argument giving the first maximum is evidently larger than that for the azimuthal component, strongly confirming the assumption that the horizontal motion is polarized perpendicularly. By identifying the zeros, maxima and minima of this curve with those of $J_0(x)+J_2(x)$ given in Table I, we can obtain wave velocities for various frequencies as shown in Fig. 17 by the mark $\times$.

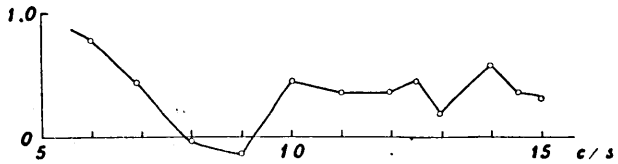

Fig. 15. $\rho(\omega_0, r)$, for $r=7.5$ m, plotted against ω_0.

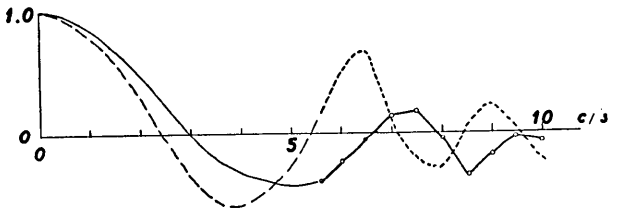

Fig. 16. Comparison of correlation curves for azimuthal and radial components.

Fig. 17 clearly indicates that all the points obtained from three independent measurements are concentrated fairly well to form a single smooth curve. This fact shows the validity of our assumption that the predominant wave in the horizontal motion of the microtremors is the one having a single definite velocity for a given frequency and being

polarized in the direction perpendicular to that of propagation. In short, the predominant wave is of Love type and the curve in Fig. 17 is its dispersion curve.

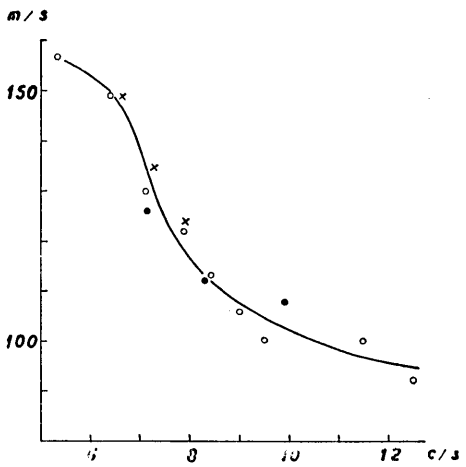

Fig. 17. Dispersion curve of horizontal motion.

6. Vertical motions

A similar measurement as applied to the horizontal motion is made about the vertical motion also along the line segment QR. It is evident that there is no polarization with respect to the vertical motion in the case of two dimensional waves. Therefore, if a wave having a definite velocity corresponding to a given frequency is predominant in the vertical motion, the autocorrelation coefficient will take the form,

$$\rho(r,\ \omega_0)=J_0\left(\frac{\omega_0}{c(\omega_0)}r\right),$$

which was derived in section 6, Chapter 1. The zeros, maxima, and minima of $J_0(x)$ are given in Table II.

The result of measurement is shown in Fig. 18, where the correlation is taken between two vertical seismometers placed along QR and

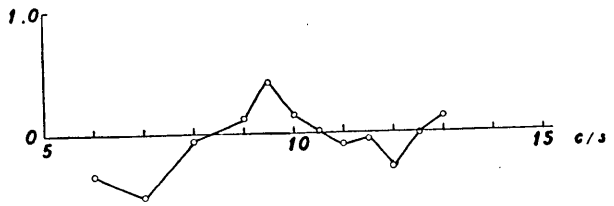

Fig. 18. $\rho(\omega_0, r)$ of vertical motion, for r=25m, plotted against ω_0.

25 m apart from each other. It is confirmed, by observing correlations for a fixed frequency and various distances, that the maximum of the correlation curve of the wave at the frequency 9.5 c/s is the first maximum, and the minimum at 7.0 c/s is the first minimum. From the

figure it can be seen that the values of the first maximum and the first minimum are almost equal to those of $J_0(x)$. Thus we may assume that a surface wave in the narrow sense is predominant in the

Table II. $J_0(x)$.

	x	$J_0(x)$		x	$J_0(x)$
1st zero	2.40	0	2nd min	10.18	−0.250
1st min.	3.83	−0.403	4th zero	11.79	0
2nd zero	5.52	0	2nd max.	13.33	+0.218
1st max.	7.01	+0.300	5th zero	14.93	0
3rd zero	8.65	0			

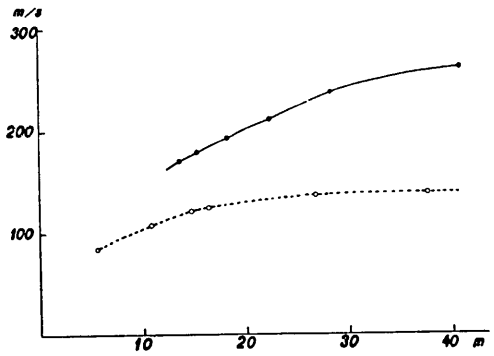

Fig. 19. Comparison of dispersion curves of vertical motion obtained from experiment and theory. (Abscissa is wave length.)

vertical motion as well as in the horizontal motion. By identifying the zeros, maxima and minima of the curve in Fig. 18 with those of $J_0(x)$, we get a dispersion curve as shown by a full line in Fig. 19.

If the vertical motion is a surface wave in the narrow sense, it is most natural to regard it as of Rayleigh type. It is remarkable that the wave velocity for the vertical motion identified as a Rayleigh wave is about twice as large as that for the horizontal motion identified as a Love wave, as indicated in Figs. 17 and 19.

7. The velocity of S wave at various depths

Recently T. Takahashi[16] (1955) studied the dispersion of Love type waves propagating over a heterogeneous medium, and gave a method of determining the structure of the medium from a given dispersion curve. According to him, if the derivatives of density and rigidity are zero at the surface, the depth z at which the velocity of S wave is equal to a given V_S can be found by the formula

$$Z(V_S)=\frac{1.11}{4\pi}V_S\int_0^{T_S}\left[\left\{\frac{V_S}{V_Q(T)}\right\}^2-1\right]^{-1/2}dT$$

16) T. TAKAHASHI, *Bull. Earthq. Res. Inst.*, **33** (1955), 287.

where T is the period of wave, $V_Q(T)$ is the phase velocity of wave corresponding to a period T, and T_S is the period for which $V_Q(T)$ is equal to V_S.

Introducing the phase velocity of the horizontal motion given in Fig. 17 into the above formula, we get the variation of S wave velocity with depth as shown in Fig. 20. In this calculation, the surface values of the velocity and its derivative are assumed as 75 m/s and zero respectively. From Fig. 20 it can be seen that there is a rapid increase in velocity at depths from 2 m to 3.5 m, and above and below these depths the velocities are nearly constant respectively. This fact suggests a discontinuity of substance at the depth of about 2.7 m.

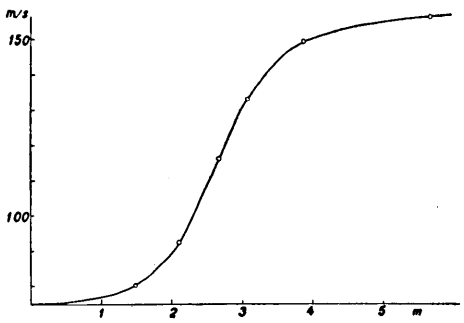

Fig. 20. Velocity of S wave at depths.

The dispersion curve of Rayleigh waves propagating over a layered surface was discussed by K. Sezawa[17] (1927), and was shown graphically in the case of $\lambda=\mu$, $\lambda'=\mu'$, and $\rho=\rho'$. If we assume a layer having thickness of 2.7 m with the velocity of S wave of 75 m/s, and a substratum with 160 m/s as suggested from the curve in Fig. 20, an application of Sezawa's result to such a structure yields a dispersion curve for Rayleigh wave as shown by a dotted line in Fig. 19. The figure shows a considerable discrepancy between the curve obtained by the measurement and that expected theoretically from the structure which is determined by the use of the dispersion curve of the Love wave.

This discrepancy may be attributed either to the difference between the velocity of the SV wave and that of the SH wave, or to a misidentification of the type of wave.

A similar phenomenon is reported in a paper by J. E. White, S. N. Heaps, and P. L. Lawrence[18] (1956) in which a surface wave identified as Rayleigh wave is shown to have group and phase velocities about twice as large as those for Love wave.

17) K. SEZAWA, *Bull. Earthq. Res. Inst.*, **3** (1927), 1~18.
18) J. E. WHITE, S. N. HEAPS, and P. L. LAWRENCE, *Geophysics*, **21** (1956), 715.

8. An example of anomalous dispersion

In this section will be given the result of measurement along the line segment PQ in the tennis court as shown in Fig. 9. As has often been mentioned previously, this place is covered by hard surface soil. Fig. 21 indicates the autocorrelation coefficients with respect to waves filtered by resonators having frequencies 7.5, 13.6, 14.6 and 21.2 c/s. In this case the coefficients are plotted against the distance between the seismometers. The seismometers used are of horizontal type and are placed so as to be sensitive in the direction perpendicular to the line PQ. Accordingly the autocorrelation curves shown in Fig. 21 correspond to the azimuthal component. If such a polarized wave as found in the horizontal motion along the line segment QR is also predominant in this case, the form of the curves in Fig. 21 must coincides with that of $J_0(x)-J_2(x)$. This coincidence, however, is not well established, perhaps due to the horizontal heterogeneity of the surface soil.

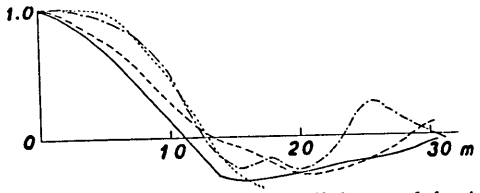

Fig. 21. Autocorrelation coefficients of horizontal motion along the line PQ for
$\omega_0=7.5$ ·····,
$\omega_0=13.6$ —·—·—,
$\omega_0=14.6$ – – – –,
and $\omega_0=21.2$ ————.

The most striking fact revealed by this measurement is that the general trend of the curves or the distance giving their first zero is almost independent of the frequency. This fact reminds us the type D illustrated in the preliminary discussions. But to be consistent with the existence of wave of type A at a near place, it may be more natural to attribute this fact to the effect of hard surface soil and to assume an anomalous dispersion in which the wave velocity increases almost proportionally to the frequency of vibration.

The autocorrelation coefficients of vertical motions having frequencies of 7.0 and 13.6 c/s are plotted against the distance in Fig. 22. Although the curve for the frequency 13.6 c/s indicates the existence of waves having shorter wave lengths, the general trend coincides with that for the fre-

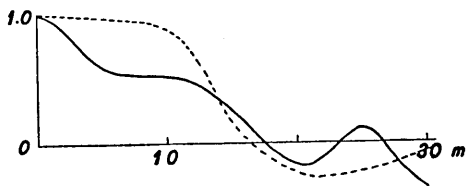

Fig. 22. Autocorrelation coefficients of vertical motion along the line PQ for
$\omega_0=13.6$ c/s ————,
and $\omega_0=7.0$ c/s – – – – –.

quency 7.0 c/s, also showing an anomalous dispersion.

From the comparison between the curves for the horizontal motions and those for the vertical motions, it can be seen that the velocity of the latter is notably larger than that of the former, and this is the very fact observed along the line segment QR.

9. Unusual behavior of vibration of 6.0 c/s on a storm day

On March 9, 1957, when it was stormy due to a low pressure passing near the east coast of Japan, filtration and correlation analyses were applied to the vibrations of two horizontal seismometers placed at the points S and T in Fig. 9. The range of the resonator frequency was from 5.5 to 10.0 c/s. The correlation coefficients obtained are plotted in Fig. 23 against the frequency of the resonator.

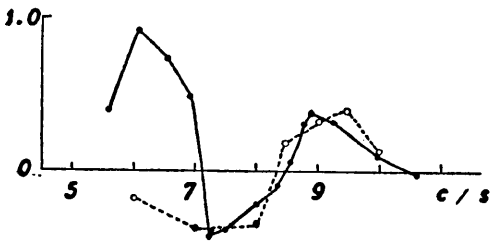

Fig. 23. Comparison of correlation curves measured on a storm day and a calm day.

The dotted curve in Fig. 23 indicates the correlation observed on a calm day. The coincidence of these two curves is fairly good in the frequency range higher than 7.5 c/s, but the value of correlation coefficient for the storm day at the frequency 6.0 c/s amounts to more than 0.9, while that for the calm day is below zero. This high value was unexpected, for the distance between seismometers is about 14 m which is long enough for a considerable decrease of correlation with respect to vibrations having higher frequencies than 5.0 c/s. Also this fact is interesting because the frequency of 6.0 c/s is just twice as large as the most predominant frequency of microtremors at this place, and it suggests to us a possibility that the vibration of type B mentioned in the preliminary discussions might be generated under some circumstances. Further study of this problem is being prepared.

10. Discussions and summary

The application of our method to the microtromors has satisfactorily revealed the nature of microtremors in the frequency range higher than 5.0 c/s, and yielded the following results.

1. In the horizontal motion of microtremors a perpendicularly po-

larized wave is predominant. Both the horizontal and vertical motions can be regarded as having respectively a single definite velocity corresponding to a given frequency.

2. Identifying the horizontal motion as Love wave, we have obtained the velocity of S wave at various depths.

3. The vertical motion also shows a definite dispersion. But if we identify it as Rayleigh wave in a layered medium, the obtained phase velocity becomes about twice as large as that expected theoretically from the velocity of S wave at depths which is determined by the use of dispersion curve for Love wave.

4. The microtremors show a marked anomalous dispersion at a place having hard surface soil.

It may be noted that the value of velocity obtained by our method is that of the phase velocity, so that the corresponding dispersion curve indicates the local structure of medium at the place of measurement. In addition, there is no such ambiguity in our method as that encountered in the determination of travel time of surface waves by the customary method.

The results obtained in this chapter strongly show the efficiency of the present method for the analyses of complicated waves. We shall note here several ways of its application to other waves appearing in Seismology.

Our method will be most effectively applied to the microseismic waves, and will clarify its wave type, the direction of propagation, and the structure of medium at the place of measurement just in the same way as in the present study of microtremors. The location of the origin of volcanic tremors is a very interesting problem in physical volcanology and can be most easily and precisely made by the direction determination by our method. In addition, the coda part of seismic waves due to an earthquake will be another important object to be studied by our method. The investigations of this coda part will give us additional informations about the structure of medium through which the wave is propagated.

Another important problem is the location of the epicentres of very small earthquakes. The direction of wave propagation determined by the present method together with the time of $P-S$ duration will enable us to locate epicentres from observations made at a single station.

11. Acknowledgment

The writer expresses his thanks to Prof. Chuji Tsuboi of the Geophysical Institute, Tokyo University for his constant guidance and encouragement as well as for his valuable suggestions made in the preparation of the manuscript. The greater part of this study was made while the writer was working at the Geophysical Institute. This work was supported in part by a Grant from the Ministry of Education.

---

22. 複雑な波動のスペクトル的研究

地震研究所　安芸敬一

ここで複雑な波動というのは，stationary stochastic wave と呼ぶべきものである．これまで地震記象は位相的な立場から主に解析されて来ているが，位相的には取扱い得ない波動も地震学の分野には数多くある．たとえば，地震波のなかの複雑な部分，脈動，常時微動，火山微動などである．こういう波動の理論模型は stationary stochastic wave と呼ぶのが適当なものであり，このような波動について，1 次元及び 2 次元の場合，その空間スペクトルと時間スペクトルの関係を求めた．

このような波の解析は，先づ sharp な filter をとおし，次に空間相関を測定するという手続きによつて最も有効に行われる．このための電子管装置を製作した．

この方法を常時微動に応用した結果次のことがわかつた．但し観測された常時微動は本郷向ケ丘のものであり．周波数範囲は 5 c/s 以上である．

1) 常時微動はあらゆる方向について殆んど一様な強さをもつている．

2) 上下動も水平動も，周波数を与えると速度が殆んど 1 つに定まる．佐藤泰夫のいう狭い意味での表面波である．

3) 上下動も水平動も分散性をもつ．

4) 水平動は主に進行方向に対し直角に振動する波から成る．つまり Love 波と見做される．

5) 分散曲線から地下の S 波の速度を高橋健人の方法によつて求めた．

6) 上下動の速度は水平動のそれの略 2 倍の大きさをもつ．この事実は White 等によつても経験されているが，理論的には不可解であると思われる．

7) 固い地表層をもつ場所で常時微動は逆分散の現象を示した．速度が殆んど周波数に比例して増大する．
